


# Activation of the prostaglandin E<sub>2</sub> EP<sub>2</sub> receptor attenuates renal fibrosis in unilateral ureteral obstructed mice and human kidney slices

Michael Schou Jensen<sup>1</sup> | Henricus A. M. Mutsaers<sup>1</sup> | Stine Julie Tingskov<sup>1</sup> |  
Michael Christensen<sup>1</sup> | Mia Gebauer Madsen<sup>2</sup> | Peter Olinga<sup>3</sup> | Tae-Hwan Kwon<sup>4</sup> |  
Rikke Nørregaard<sup>1</sup> 

<sup>1</sup>Department of Clinical Medicine, Aarhus University, Aarhus, Denmark

<sup>2</sup>Department of Urology, Aarhus University Hospital, Aarhus, Denmark

<sup>3</sup>Department of Pharmaceutical Technology and Biopharmacy, University of Groningen, Groningen, the Netherlands

<sup>4</sup>Department of Biochemistry and Cell Biology, School of Medicine, Kyungpook National University, Daegu, Korea

## Correspondence

Rikke Nørregaard, Department of Clinical Medicine, Aarhus University, Palle Juul-Jensens Boulevard 99, DK-8200 Aarhus N., Denmark.

Email: RN@clin.au.dk

## Funding information

Hildur and Dagny Jacobsens Foundation, Grant/Award Number: 1295716-1; Lundbeckfonden, Grant/Award Number: R231-2016-2344; Det Frie Forskningsråd, Grant/Award Number: 6110-00231B; Aarhus Universitets Forskningsfond, Grant/Award Number: AUFF-E-2015-FLS-8-69

See Editorial Commentary: Sands, J. M. 2019. Translating kidney fibrosis: Role of the EP<sub>2</sub> receptor. *Acta Physiol.* 227, e13318.

## Abstract

**Aim:** Renal fibrosis plays a pivotal role in the development and progression of chronic kidney disease, which affects 10% of the adult population. Previously, it has been demonstrated that the cyclooxygenase-2 (COX-2)/prostaglandin (PG) system influences the progression of renal injury. Here, we evaluated the impact of butaprost, a selective EP<sub>2</sub> receptor agonist, on renal fibrosis in several models of kidney injury, including human tissue slices.

**Methods:** We studied the anti-fibrotic efficacy of butaprost using Madin-Darby Canine Kidney (MDCK) cells, mice that underwent unilateral ureteral obstruction and human precision-cut kidney slices. Fibrogenesis was evaluated on a gene and protein level by qPCR and Western blotting.

**Results:** Butaprost (50 μM) reduced TGF-β-induced fibronectin (FN) expression, Smad2 phosphorylation and epithelial-mesenchymal transition in MDCK cells. In addition, treatment with 4 mg/kg/day butaprost attenuated the development of fibrosis in mice that underwent unilateral ureteral obstruction surgery, as illustrated by a reduction in the gene and protein expression of α-smooth muscle actin, FN and collagen 1A1. More importantly, a similar anti-fibrotic effect of butaprost was observed in human precision-cut kidney slices exposed to TGF-β. The mechanism of action of butaprost appeared to be a direct effect on TGF-β/Smad signalling, which was independent of the cAMP/PKA pathway.

**Conclusion:** In conclusion, this study demonstrates that stimulation of the EP<sub>2</sub> receptor effectively mitigates renal fibrogenesis in various fibrosis models. These findings warrant further research into the clinical application of butaprost, or other EP<sub>2</sub> agonists, for the inhibition of renal fibrosis.

## KEYWORDS

butaprost, cyclooxygenase-2, precision-cut kidney slices, prostaglandin E<sub>2</sub> receptor, renal fibrosis

Michael Schou Jensen and Henricus A. M. Mutsaers contributed equally to this study.

This is an open access article under the terms of the Creative Commons Attribution License, which permits use, distribution and reproduction in any medium, provided the original work is properly cited.

© 2019 The Authors. *Acta Physiologica* published by John Wiley & Sons Ltd on behalf of Scandinavian Physiology Society

## 1 | INTRODUCTION

Chronic kidney disease (CKD) affects approximately 10% of the adult population in developed countries.<sup>1</sup> Moreover, the global incidence of CKD is on the rise, and as a consequence the disease greatly impacts health care budgets. Renal fibrosis, which is characterized by the excessive production and deposition of extracellular matrix proteins by activated myofibroblasts, plays a pivotal role in the development and progression of CKD as well as in renal transplant failure.<sup>2</sup> Fibrosis results in the loss of organ architecture and function, and is regarded as the most damaging process in CKD; yet, despite overwhelming efforts, effective therapeutic targets have not been identified. Thus, an urgent and unmet clinical need remains.

Previously, it has been demonstrated that the cyclooxygenase-2 (COX-2)/prostaglandin (PG) system plays a dominant role in the progression of renal injury.<sup>3-5</sup> COX enzymes catalyze the conversion of arachidonic acid into prostaglandins, including prostaglandin E<sub>2</sub> (PGE<sub>2</sub>), which is an important mediator of numerous physiological processes in the kidney, including renal hemodynamics as well as water and salt balance.<sup>3</sup> PGE<sub>2</sub> exerts its biological activity by activating several G protein-coupled prostanoid receptors, known as EP<sub>1</sub>-EP<sub>4</sub>.<sup>6</sup> Several studies have demonstrated an important role for the EP<sub>1</sub>-EP<sub>4</sub> receptors in renal injury. Previously, it has been reported that EP<sub>1</sub> deletion in mice reduced diabetes-induced expression of the fibrotic markers fibronectin and  $\alpha$ -actin.<sup>7</sup> Furthermore, EP<sub>1</sub> antagonism, using ONO8711, decreased fibronectin (FN) expression in mouse proximal tubule cells.<sup>7</sup> In addition, deletion of EP<sub>2</sub> increases baseline systolic blood pressure and causes salt-sensitive hypertension, which is a known risk factor for renal damage.<sup>8</sup> Interestingly, renal gene expression of both EP<sub>2</sub> and EP<sub>4</sub> is shown to be increased during renal fibrogenesis, suggesting that these receptors might play a protective role in the fibrotic process.<sup>4,9</sup> This notion is supported by the fact that butaprost, a selective EP<sub>2</sub> agonist, inhibits TGF- $\beta$ 1-induced myofibroblast transition of human foetal lung fibroblasts.<sup>10</sup> However, the efficacy of butaprost for the treatment of renal fibrosis remains to be elucidated.

In the current study, we investigated the impact of butaprost on renal fibrogenesis at the cell, tissue and organ levels using well-established *in vitro* and *in vivo* models as well as a recently developed human model of renal fibrosis, *viz.* precision-cut kidney slices (PCKS). This model is suitable for studying multicellular (pathological) processes, *eg.* fibrosis, directly in human tissues since cellular heterogeneity as well as organ architecture are maintained in the slices.

## 2 | RESULTS

### 2.1 | The EP<sub>2</sub> agonist, butaprost, mitigates TGF- $\beta$ -induced epithelial-mesenchymal transition (EMT)

EMT is an integral part of the fibrotic process. Therefore, we evaluated the impact of butaprost on TGF- $\beta$ -induced EMT in Madin-Darby Canine Kidney (MDCK) cells, which express the EP<sub>2</sub> receptor (Figure 1A). As shown in Figure 1B, exposure of MDCK cells to TGF- $\beta$  caused a fourfold increase in FN protein expression, which was concentration-dependently inhibited by butaprost. At the highest tested concentration (50  $\mu$ M), butaprost almost completely blocked TGF- $\beta$ -induced FN expression. Therefore, this concentration was used for the remainder of the study. In addition, Figure 1 demonstrates that treatment with TGF- $\beta$  increased TGF- $\beta$  gene expression, stimulated Smad2 phosphorylation and induced a spindle-like morphology indicative of EMT, all of which could be inhibited by butaprost. Taken together, these findings indicate that butaprost mitigates TGF- $\beta$ /Smad signalling and EMT in MDCK cells.

Next, we investigated whether butaprost mitigated the profibrotic effects of TGF- $\beta$  via the cAMP pathway, which has been shown to play a role in pulmonary fibrosis.<sup>10</sup> It has been demonstrated that activation of the EP<sub>2</sub> receptor increases intracellular cAMP levels.<sup>3</sup> Indeed, treatment with butaprost markedly increased intracellular cAMP levels; however, this response was suppressed in presence of TGF- $\beta$  (Figure 2A). Since butaprost clearly affected cAMP levels, we evaluated whether this effect was due to changes in adenylate cyclase (AC) activity, the enzyme that converts ATP into cAMP. As shown in Figure 2B, exposure of MDCK cells to a combination of TGF- $\beta$ , butaprost and SQ22536 (an AC inhibitor) did not hamper the anti-fibrotic effect of butaprost.

As inhibition of AC did not attenuate the effects of butaprost, we investigated if protein kinase A (PKA), the cAMP-dependent activator of cAMP response element-binding protein (CREB), was involved in its activity. Exposure of MDCK cells to a combination of TGF- $\beta$ , butaprost and H89 (a PKA inhibitor) did not reverse the anti-fibrotic effect of butaprost (Figure 2C). These findings suggest that the impact of butaprost on fibrogenesis is unconstrained by the cAMP/PKA signalling pathway.

### 2.2 | Butaprost attenuates unilateral ureteral obstruction (UUO)-induced fibrosis in mice

Butaprost clearly reduced fibrogenesis in MDCK cells; therefore, we studied the anti-fibrotic efficacy of this compound in a murine *in vivo* model of renal fibrosis, namely UUO. Following surgery, we did not observe any

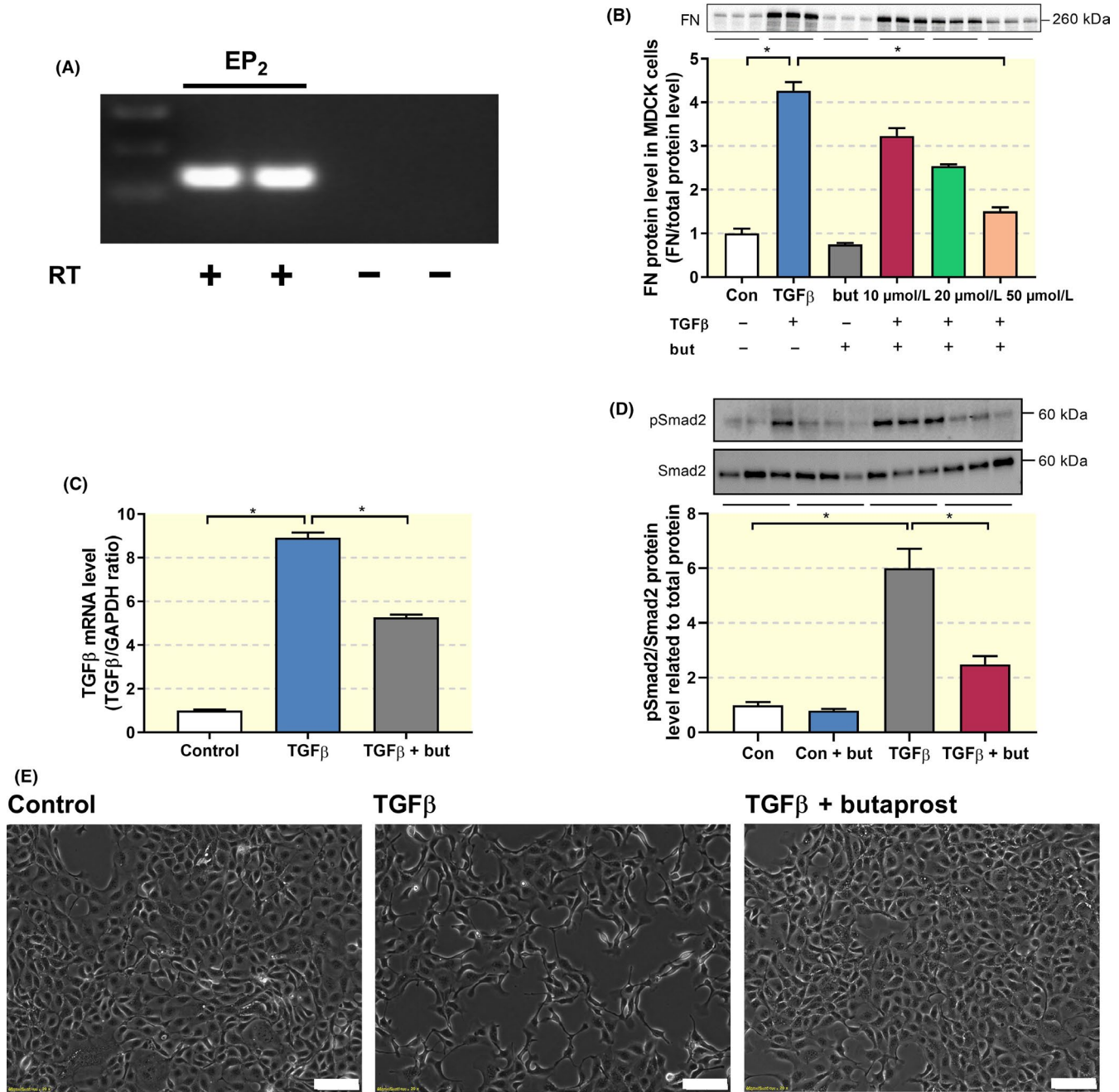


**FIGURE 1** Butaprost attenuates TGF- $\beta$ -induced epithelial-mesenchymal transition. (A) Gene expression was studied by RT-PCR with (+) or without (-) reverse transcriptase (RT) enzyme. (B) MDCK cells were exposed to 5 ng/ml TGF- $\beta$  in the absence or presence of butaprost (10-50  $\mu$ M) for 24 h. FN protein expression was studied using western blotting (n = 3). (C) Gene expression was studied by qPCR. Relative expression was calculated using the reference gene GAPDH (n = 6). (D) Immunoblot analysis of the expression of pSmad2/Smad2 normalized to total protein (n = 6). (E) Representative microscopy images showing MCKD cell morphology. 10 $\times$  magnification, scale bar is 100  $\mu$ m. Data are presented as mean  $\pm$  SEM. \**P* < 0.05

changes in body weight in the four groups. However, the obstructed kidney from UUO mice appeared to be swollen and was increased in weight as compared to sham mice (Table 1). Administration of butaprost did not affect the weight of the obstructed kidney. In addition, plasma creatinine, BUN as well as plasma sodium and potassium did not change between the four groups (Table 1). Next, we

confirmed the presence of the EP<sub>2</sub> receptor in the model using both qPCR and immunohistochemistry. After seven days of UUO, expression of the EP<sub>2</sub> receptor markedly increased, both on mRNA and protein level (Figure 3). However, this was not significantly altered by butaprost treatment. Immunohistochemical staining of kidney sections revealed that EP<sub>2</sub> receptor immunoreactive protein

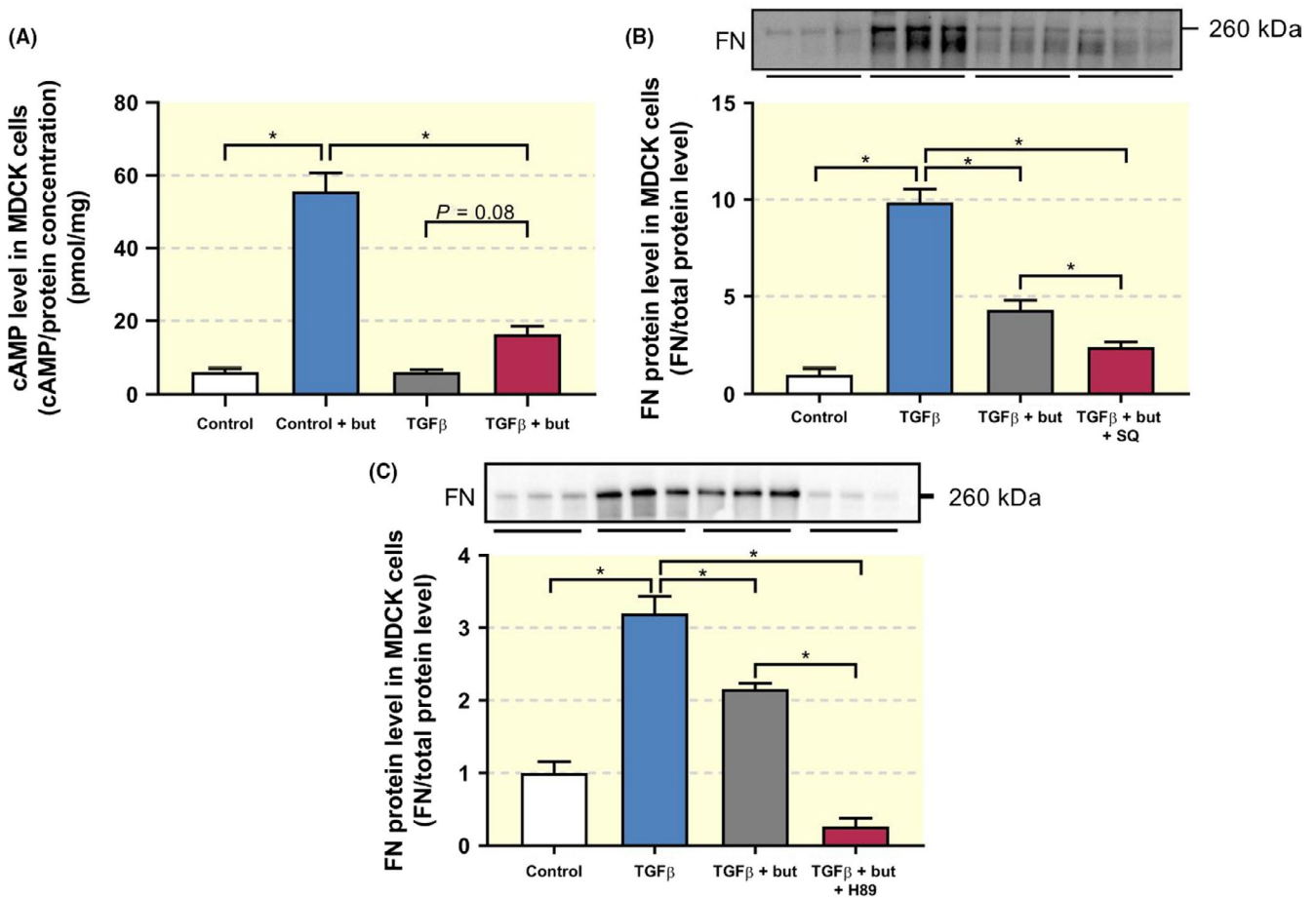


**FIGURE 2** Anti-fibrotic effect of butaprost is independent of cAMP/PKA signalling. MDCK cells were exposed to 5 ng/ml TGF- $\beta$  in the absence or presence of butaprost (50  $\mu$ M), SQ22536 (75  $\mu$ M) or H89 (10  $\mu$ M) for 24 h. (A) cAMP levels were determined in cell lysates via ELISA (n = 6). (B, C) FN protein expression was studied using western blotting (n = 5-6). Data are presented as mean  $\pm$  SEM. \* $P$  < 0.05

Groups	Sham	Sham + butaprost	UUO	UUO + butaprost
Bodyweight (BW) (g)	22.2 $\pm$ 0.6	22.8 $\pm$ 0.3	22.1 $\pm$ 0.5	22.1 $\pm$ 0.3
Obstructed kidney/BW (mg/mg mice)	5.8 $\pm$ 0.1	6.3 $\pm$ 0.3	7.5 $\pm$ 0.4*	8.4 $\pm$ 0.1 <sup>#</sup>
Creatinine ( $\mu$ mol/L)	11.7 $\pm$ 0.8	10.6 $\pm$ 0.8	12.8 $\pm$ 1	11.3 $\pm$ 0.6
BUN (mmol/L)	7.5 $\pm$ 0.2	6.3 $\pm$ 0.4	8.7 $\pm$ 0.6	7.7 $\pm$ 0.5
Na (mmol/L)	149.6 $\pm$ 0.6	149.5 $\pm$ 0.5	150 $\pm$ 0.7	149.8 $\pm$ 0.4
K (mmol/L)	4.8 $\pm$ 0.1	4.8 $\pm$ 0.3	4.4 $\pm$ 0.1	4.5 $\pm$ 0.1

Values are presented as mean  $\pm$  SEM. Sham: n = 6, sham + butaprost: n = 6, UUO: n = 8 and UUO + butaprost: n = 10.

\* $P$  < 0.05 compared to sham;

<sup>#</sup> $P$  < 0.05 compared to sham + butaprost.

**TABLE 1** Functional data after UUO and butaprost treatment

was stronger in the UUO kidneys, as compared to sham-operated mice, and localized to the interstitial cells (Figure 3C). To examine whether the increased EP<sub>2</sub> receptor labelling was associated with myofibroblasts in the interstitium, we performed double immunofluorescent labelling with

antibodies against the EP<sub>2</sub> receptor (red) and the myofibroblast marker  $\alpha$ SMA (green) in the obstructed kidney. As shown in Figure 4, EP<sub>2</sub> receptor expression co-localizes with  $\alpha$ SMA indicating that the EP<sub>2</sub> receptor is associated with interstitial myofibroblasts.

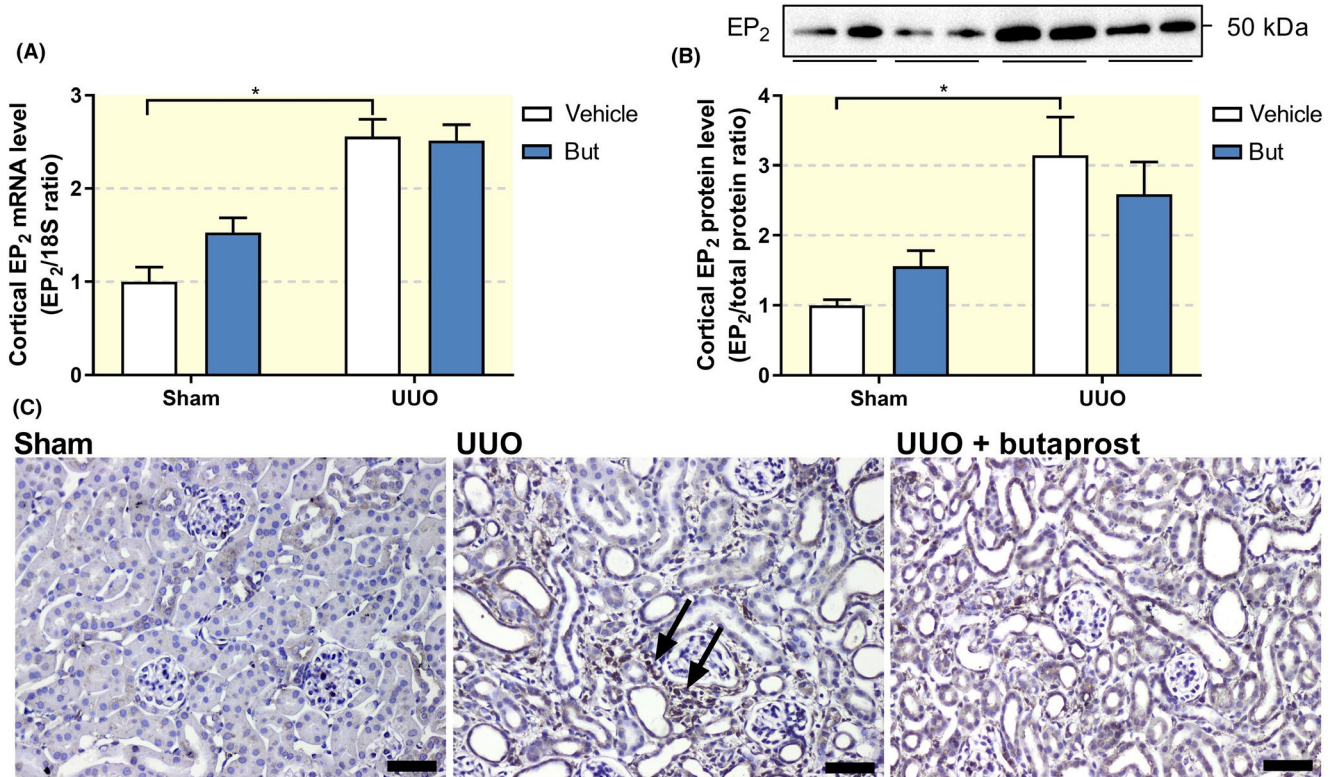


**FIGURE 3** Impact of UUO and butaprost on EP<sub>2</sub> receptor expression in vivo. Mice were subjected to 7 days of UUO and treated with butaprost (4 mg/kg). (A) Gene expression was studied by qPCR. Relative expression was calculated using the reference gene 18S (n = 6-10). (B) Cortical EP<sub>2</sub> protein expression was studied using western blotting (n = 6-10). (C) Representative immunohistochemistry images showing EP<sub>2</sub> expression. 20× magnification, scale bar is 50 μm. Arrows indicate EP<sub>2</sub>-positive interstitial cells. Data are presented as mean ± SEM. \**P* < 0.05

Regarding the development of fibrosis, we observed a clear increase in the protein expression of FN and αSMA following UUO, and treatment with butaprost reverted the expression to sham levels (Figure 5A,B). Furthermore, qPCR revealed that 7 days of UUO caused a 25-fold increase in the gene expression of αSMA, a 17-fold increase in FN gene expression and a 15-fold increase in COL1A1 gene expression. Treatment with butaprost significantly reduced the mRNA levels of both αSMA and COL1A1 (Figure 5C-E). In accordance, fluorescence microscopy revealed that UUO resulted in increased αSMA staining, which could be mitigated by treatment with butaprost (Figure 5F). Furthermore, as shown in Figure 5G-I, UUO increased both interstitial and tubular volume, indicative of renal damage, which was prevented by butaprost treatment. Thus, stimulation of the EP<sub>2</sub> receptor attenuates UUO-induced renal fibrosis in mice.

### 2.3 | Stimulation of the EP<sub>2</sub> receptor mitigates fibrogenesis in human PCKS

Finally, we investigated whether the anti-fibrotic effect of butaprost could also be observed in a novel translational fibrosis model, *viz.* human PCKS. As shown in Figure 6,

treatment with 10 ng/ml TGF-β for 48 hours induced a fibrotic response in the slices, resulting in a more than four-fold increase in the gene expression of COL1A1, FN and αSMA (Figure 6A-C), without affecting PCKS viability as evaluated by ATP measurements (Figure 6D). In addition, exposure to TGF-β increased mRNA levels of the EP<sub>2</sub> receptor, in line with the results obtained in UUO mice (Figure 7A). Moreover, qPCR revealed that butaprost significantly antagonized TGF-β-induced fibrogenesis, as illustrated by a reduced expression of all tested fibrosis markers (Figure 7C-E) without affecting PCKS viability (Figure 7B). To exclude the possibility that endogenous prostaglandins elicited the anti-fibrotic effects contributed to butaprost we performed several experiments in the presence of indomethacin, an inhibitor of both COX-1 and COX-2. Our results demonstrated that butaprost, in the absence of endogenous prostaglandins, still attenuated TGF-β-induced fibrogenesis (Figure 7F). In addition, fluorescence microscopy showed stronger αSMA staining in PCKS exposed to TGF-β. Administration of butaprost and TGF-β in combination diminished staining intensity as compared to treatment with TGF-β alone (Figure 7G). Thus, butaprost also attenuates TGF-β-induced fibrogenesis in a human model of renal fibrosis.

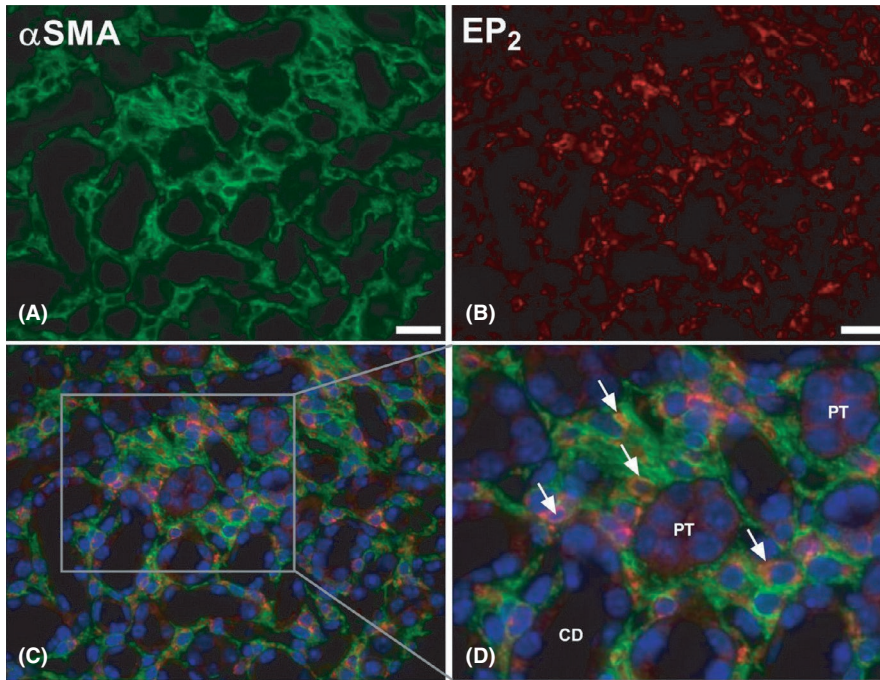


**FIGURE 4** Expression of the EP<sub>2</sub> receptor in fibrotic renal tissue. Mice were subjected to 7 days of UUO. Afterwards, the UUO kidney was harvested and used for fluorescence microscopy. Representative image of immunolabeling for (A)  $\alpha$ SMA (green) and (B) the EP<sub>2</sub> receptor (red). (C, D) Representative image of co-immunolabeling ( $\alpha$ SMA, green; EP<sub>2</sub> receptor, red) counterstained with DAPI (blue). 40 $\times$  magnification, scale bar is 20  $\mu$ m. Arrows indicate EP<sub>2</sub>-positive myofibroblasts. CD = collecting duct, PT = proximal tubule

### 3 | DISCUSSION

Renal fibrosis plays a pivotal role in the development and progression of CKD as well as in renal transplant failure. As a result, many strategies have been developed in the hope of slowing down or even reversing the fibrotic process. Even though several studies have been successful at the pre-clinical level, only limited advances have been made in the translation of these findings to the level of patient treatment.<sup>11</sup> The search for effective therapies is mainly hampered by the absence of relevant translational models of renal fibrosis. Here, we investigated the anti-fibrotic efficacy of butaprost, a selective EP<sub>2</sub> receptor agonist, using various renal fibrosis models including a recently developed human model of the disease, *viz.* PCKS.

Using a bottom-up translational approach, we demonstrated that butaprost successfully mitigated fibrogenesis in MDCK cells, UUO mice and human PCKS. To date, only a few studies have demonstrated renal protective effects of butaprost on a cellular level and, to the best of our knowledge, we are the first to unveil the positive effects of butaprost in a multicellular human PCKS model as well as in an *in vivo* model. On a cellular level, Liu and colleagues described that butaprost treatment prevented TGF- $\beta$ -induced injury in MPC5 mouse podocytes, as illustrated by an increased proliferation and expression of slit diaphragm genes (nephrin, podocin and CD2AP), as well as a reduction in apoptosis.<sup>12</sup> In addition, it has been demonstrated that butaprost reduced TGF- $\beta$ -induced proliferation of glomerular mesangial cells, thereby diminishing renal

injury.<sup>13</sup> Evidently, butaprost elicits protective effects in various renal cell types.

In our hands, butaprost attenuated TGF- $\beta$ -induced EMT in MDCK cells. Even though the contribution of EMT to fibrosis remains a subject of debate, phenotypic alterations reminiscent of EMT, also referred to as epithelial phenotypic changes, do play a role in the development of renal fibrosis.<sup>14-16</sup>

The beneficial effect of butaprost is not limited to the kidney. Several studies have reported that butaprost also protects against pulmonary fibrosis. Kolodtsick and colleagues demonstrated that butaprost attenuated TGF- $\beta$ -induced myofibroblast transition of IMR-90 cells.<sup>10</sup> In addition, butaprost has been shown to inhibit TGF- $\beta$ -induced CCN2/CTGF expression in lung fibroblasts.<sup>17</sup> Furthermore, it has been demonstrated that butaprost reduces collagen synthesis in rat pulmonary fibroblasts and mitigates differentiation into myofibroblasts.<sup>18</sup> Conjointly, these data indicate that butaprost appears to be a promising candidate drug for the treatment of organ fibrosis.

It is well known that stimulation of the EP<sub>2</sub> receptor leads to activation of the cAMP/PKA pathway, and also in our hands butaprost increased cAMP levels in MDCK cells. However, our results indicated that the anti-fibrotic effect of butaprost is independent of cAMP/PKA signaling. Interestingly, it has previously been demonstrated that cAMP is not necessary for butaprost-mediated aquaporin-2 membrane targeting, which was thought to be a cAMP-dependent event,<sup>19</sup> indicating that activation of the EP<sub>2</sub> receptor might also affect other pathways. Our results further revealed that butaprost attenuated fibrosis by hampering

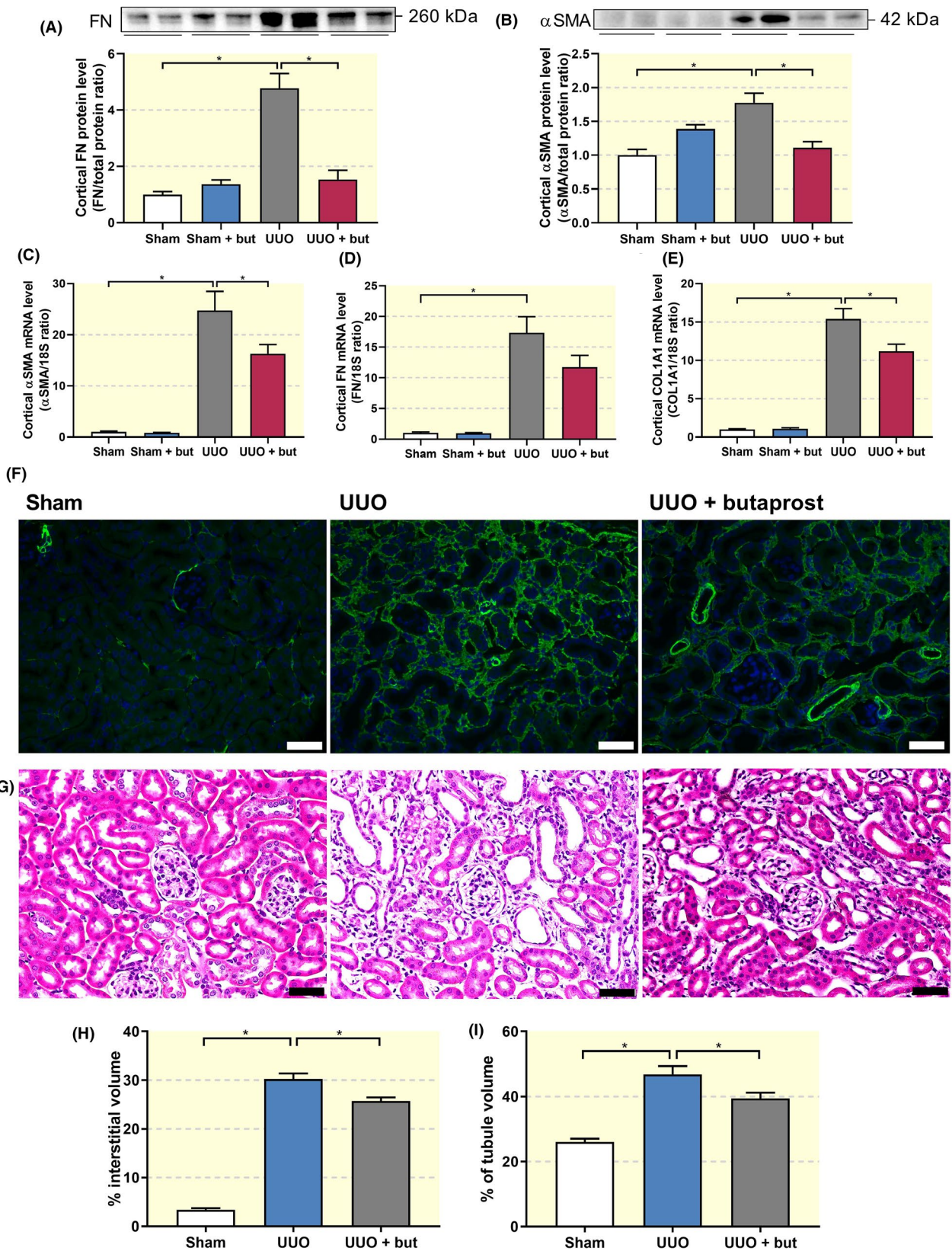


**FIGURE 5** Butaprost mitigates fibrosis in UUO mice. Mice were subjected to 7 days of UUO and treated with butaprost (4 mg/kg). (A) FN and (B) αSMA protein expression was studied using Western blot (n = 6). (C-E) Gene expression was studied by qPCR. Relative expression was calculated using the reference gene 18S (n = 6-10). (F) Representative images of immunolabeling for αSMA (green) counterstained with DAPI (blue). 20× magnification, scale bar is 50 μm. (G) Hematoxylin and eosin staining of renal cortical tissue. 20× magnification, scale bar is 50 μm. Quantification of (H) interstitial and (I) tubular volume (n = 4). Data are presented as mean ± SEM. \*P < 0.05

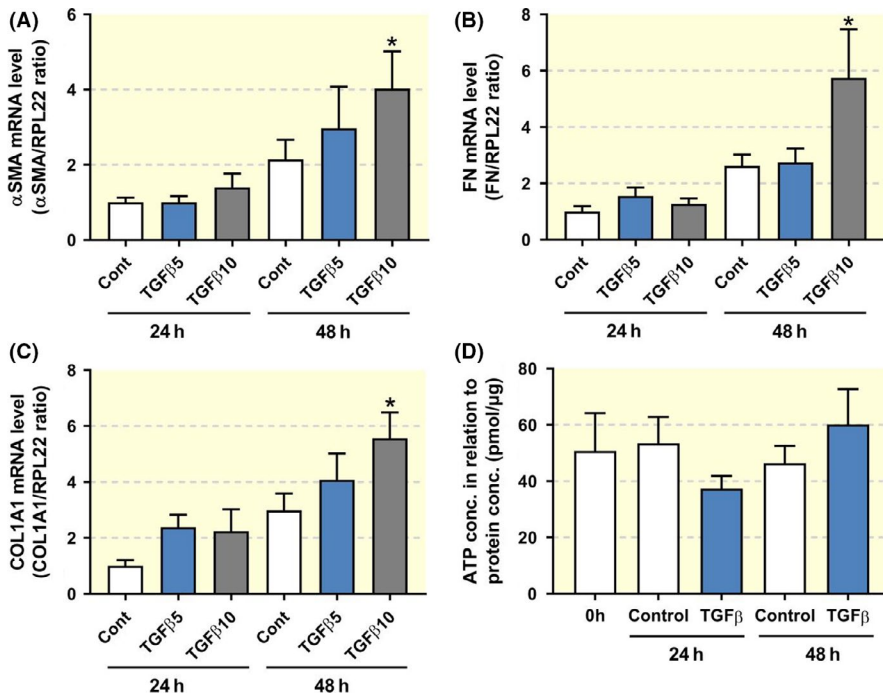


**FIGURE 6** Expression of fibrosis markers in human PCKS. PCKS were exposed to TGF- $\beta$  (5 or 10 ng/ml) for 24–48 h. (A–C) Gene expression was studied by qPCR. Relative expression was calculated using the reference gene RPL22 (n = 4–5). (D) Viability of PCKS after treatment with 10 ng/ml TGF- $\beta$ , assessed by ATP content of the slices (n = 5–7). Data are presented as mean  $\pm$  SEM. \* $P$  < 0.05

TGF- $\beta$ /Smad2 signalling. This observation is in line with the study by Neil et al, showing that PGE<sub>2</sub> reduced Smad3 expression and nuclear accumulation in normal and malignant mammary epithelial cells.<sup>20</sup> Moreover, it has been demonstrated that EP<sub>2</sub> mediates the suppressive effect of COX-2 and PGE<sub>2</sub> on TGF- $\beta$ -induced Smad2/3 signalling in normal and malignant mammary epithelial cells as well as in Balb/C mice with mammary tumours.<sup>21</sup> In addition, using human renal glomerular mesangial cells, it has been shown that PGE<sub>2</sub> induced post-translational modification of Smad2 and promoted Smad2/4 complex formation.<sup>22</sup> These findings support the notion that EP<sub>2</sub> receptor activation can directly influence TGF- $\beta$ /Smad signalling.

Here, we show that the EP<sub>2</sub> receptor is expressed in interstitial myofibroblasts following UUO. The current understanding regarding the tissue distribution of the EP<sub>2</sub> receptor is very limited. Using Northern blot analysis of mRNA expression, it has been demonstrated that the receptor is mainly present in the uterus, lung and spleen, exhibiting only low mRNA levels in the kidney.<sup>23</sup> In rabbit kidney, the receptor was detected in glomeruli, thin descending limbs of Henle's loop as well as medullary and cortical collecting ducts.<sup>24</sup> In the same study, it was reported that EP<sub>2</sub> receptor mRNA could be detected in cultured renal medullary interstitial cells.<sup>24</sup> In addition, in rat kidney, it has been shown that the EP<sub>2</sub> receptor is mainly expressed in the descending thin limb of the loop of Henle and the vasa recta of the outer medulla.<sup>25</sup> The described tissue expression is in line with the main function contributed to the EP<sub>2</sub> receptor, namely renal salt and water handling. However, the increased expression observed during

injury and the presence of the receptor in activated fibroblasts, as shown in this study, suggest an additional role in renal protection.

Stimulation of the EP<sub>2</sub> receptor causes vasodilation and increases renal blood flow (RBF).<sup>8</sup> It is known that preservation of RBF can diminish UUO-induced renal fibrosis.<sup>26</sup> Therefore, it is possible that improving RBF is one of the mechanisms underlying the renoprotective action of butaprost in vivo. Still, the main mechanisms of action seem to be a direct impact on TGF- $\beta$ /Smad signalling since the anti-fibrotic effect of butaprost was also clearly observed in models lacking RBF, *viz.* MDCK cells and hPCKS.

Our findings provide the first preclinical evidence that targeting the EP<sub>2</sub> receptor may prevent renal fibrosis, as such, the use of specific EP<sub>2</sub> agonists may reduce the occurrence of cardiovascular and renal side effects associated with systemic targeting of COX-2.

In conclusion, this study demonstrates that stimulation of the EP<sub>2</sub> receptor effectively mitigates renal fibrogenesis in various models of kidney injury, mainly by targeting TGF- $\beta$ /Smad signalling. These findings warrant further research into the clinical application of butaprost, or other EP<sub>2</sub> agonists, for the treatment of renal fibrosis.

## 4 | MATERIALS AND METHODS

### 4.1 | Ethics statement

The use of human tissue for the preparation of PCKS was approved by the Central Denmark Region Committees on



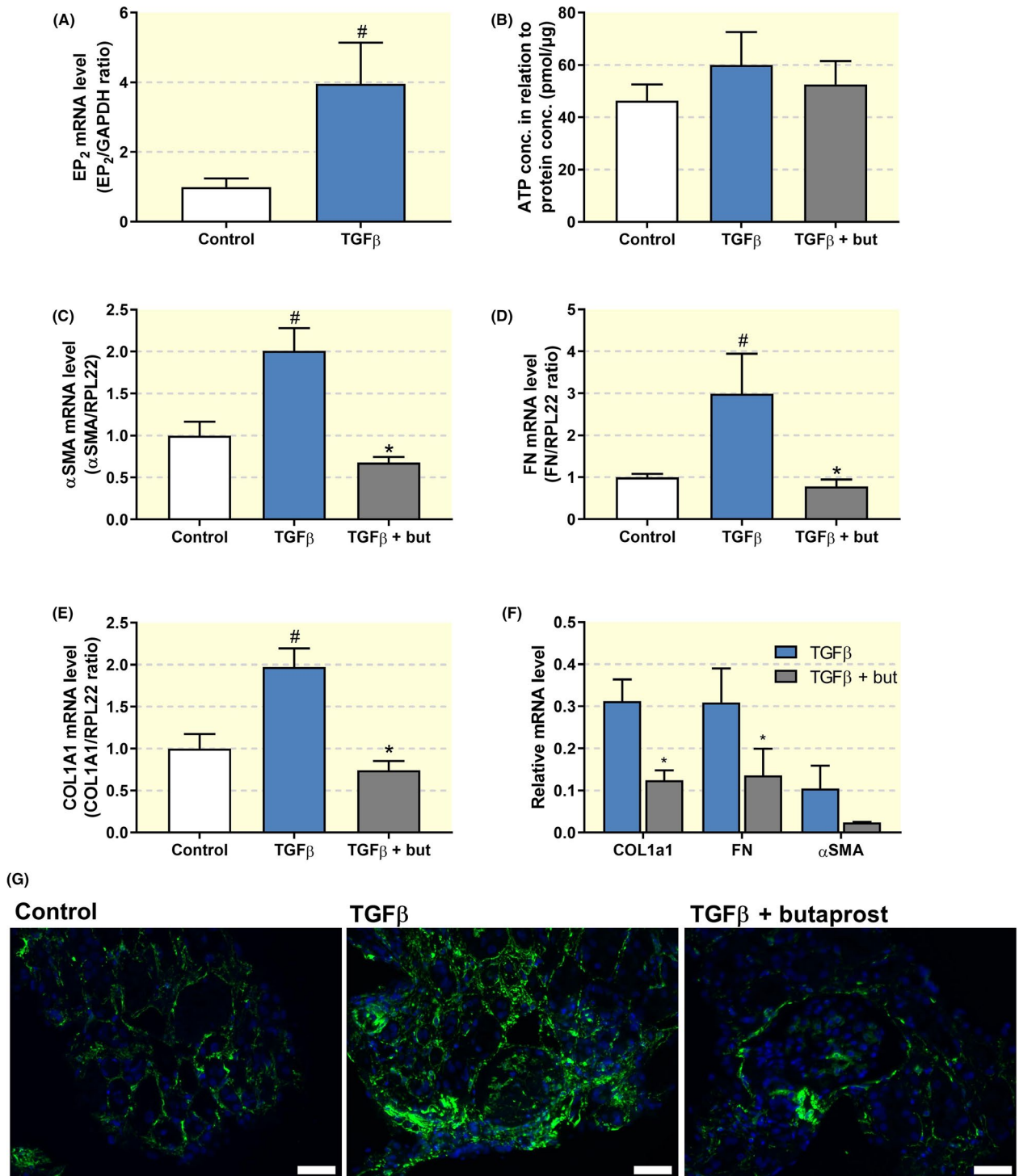


**FIGURE 7** Butaprost attenuates TGF- $\beta$ -induced fibrosis in human PCKS. PCKS were exposed to 10 ng/ml TGF- $\beta$  in the absence or presence of butaprost (50  $\mu$ M) for 48 h. (A) EP<sub>2</sub> receptor gene expression was studied by qPCR. Relative expression was calculated using the reference gene GAPDH (n = 4). (B) Viability of the slices after treatment assessed by ATP content of the slices (n = 7). (C-E) Gene expression of fibrosis markers was studied by qPCR. Relative expression was calculated using the reference gene RPL22 (n = 7). (F) PCKS were also incubated with butaprost in the presence of indomethacin (10  $\mu$ M), an inhibitor of both COX-1 and COX-2, to mitigate the influence of endogenous prostaglandins. (G) Representative images of immunolabeling for  $\alpha$ SMA (green) counterstained with DAPI (blue). 20 $\times$  magnification, scale bar is 50  $\mu$ m. Data are presented as mean  $\pm$  SEM. # and \* $P$  < 0.05 compared to control or TGF- $\beta$ , respectively

Biomedical Research Ethics (Journal number 1-10-72-211-17) and The Danish Data Protection Agency. All participants gave written informed consent.

All animal experiments were performed according to the Danish National Guidelines for animal care, and were approved by the Danish veterinary and

food administration (Approval no. 2015-15-0201-00658).

## 4.2 | Cell culture

MDCK epithelial cells were used to evaluate the anti-fibrotic efficacy of butaprost (Cayman, Cat. 13741) *in vitro*. The cells were grown in Dulbecco's Modified Eagle Medium containing 10% foetal bovine serum and 1% penicillin/streptomycin. Cells were cultured at 37°C in a 5% CO<sub>2</sub> atmosphere. Before experiments, cells were grown to 80% confluence and then serum starved for 24 h. During experiments, the cells were treated for 24 h with TGF-β (5 ng/ml), butaprost (10, 20 or 50 μM), the adenylate cyclase inhibitor SQ22536 (75 μM), the protein kinase A inhibitor H89 (10 μM) or a combination hereof. Concentrations were based on previous dose-finding studies performed in our lab. Butaprost and the inhibitors were added to the culture medium 30 min prior to exposure with TGF-β.

## 4.3 | cAMP levels

MDCK cells were cultured with and without TGF-β and butaprost for 24 h, during the last 30 min the phosphodiesterase inhibitor IBMX (0.5 mM; Sigma) was added. Afterwards, cells were lysed and intracellular cAMP levels were measured using a cAMP enzyme immunoassay kit (Sigma) according to the manufacturer's instructions. All measurements were performed in triplicate.

## 4.4 | Experimental animals

Experiments were performed using male C57BL/6 mice, 8 weeks of age and weighing 21 ± 2 g (Janvier Labs, Le Genest-Saint-Isle, France). All animals had *ad libitum* access to standard rodent chow (Altromin, Lage, Germany) and tap water. During the experiments, mice were housed in groups of 2-3 mice/cage in a 12 h:12 h light-dark cycle at a temperature of 21 ± 2°C and a humidity of 55 ± 5%. The animals were allowed to acclimatize to their cages 3-4 days prior to surgery. A preliminary dose-response study, using the following doses 1, 2 and 4 mg/kg/day, was performed using 4 animals per group. Subsequently, the anti-fibrotic effect of butaprost was validated in a larger cohort, as described below.

## 4.5 | Experimental design and surgical procedures

During surgery, mice were anesthetized with sevoflurane and placed on a heating pad to maintain an appropriate body temperature (37-38°C). Through a midline abdominal

incision, the left ureter was exposed and occluded with a 6-0 silk ligature. UUU was maintained for 7 days. A total of 30 mice were divided into 4 experimental groups: sham-operated (n = 6), sham-operated receiving butaprost (4 mg/kg/day; n = 6), 7-day UUU receiving intraperitoneal saline injections (n = 8) and 7-day UUU treated with butaprost (4 mg/kg/day; n = 10). Butaprost, diluted in saline, was administered twice daily via intraperitoneal injection starting at the day of the surgery. Dosing was based on previous dose-finding studies performed in our lab. After 7 days, the kidneys were extracted and blood was collected via cardiac puncture for further analysis. Biochemical analysis of blood samples was performed using a Roche Cobas 6000 analyzer (Roche Diagnostic) and creatinine levels were determined using the Creatinine Assay Kit (Sigma), according to the manufacturer's instructions.

## 4.6 | Precision-cut kidney slices

PCKS were prepared from functional (*ie*, eGFR > 60 ml/min/1.73 m<sup>2</sup>) and macroscopically healthy renal cortical tissue obtained from both male and female patients following tumour nephrectomies, as described previously.<sup>27</sup> In short, slices were prepared in ice-cold Krebs-Henseleit buffer, supplemented with 25 mM D-glucose, 25 mM NaHCO<sub>3</sub>, 10 mM 4-(2-hydroxyethyl)piperazine-1-ethanesulfonic acid and saturated with carbogen (95% O<sub>2</sub>, 5% CO<sub>2</sub>), using a Krumdieck tissue slicer. Subsequently, PCKS were cultured in William's E medium with GlutaMAX containing 10 mg/mL ciprofloxacin and 2.7 g/L D-(+)-Glucose solution at 37°C in an 80% O<sub>2</sub>, 5% CO<sub>2</sub> atmosphere while gently shaken. Medium was refreshed every 24 h. PCKS viability was assessed by determining the ATP content of the slices using the ATP Colorimetric/Fluorometric Assay Kit (Sigma), according to the manufacturer's instructions. Patient demographics are presented in Table 2.

## 4.7 | Western blotting

Total protein was extracted using either M-PER mammalian protein extraction reagent (cells) or RIPA buffer (kidney

**TABLE 2** Patient demographics

Gender (%male)	71.4
Age (years)	72.4 ± 5.3
BMI	24.5 ± 2.2
eGFR (ml/min/1.73 m <sup>2</sup> )	82.6 ± 7.5
Ischemia time (min)	42 ± 15

Values are presented as mean ± SD (n = 7).

BMI, body mass index; eGFR, estimated glomerular filtration rate.

**TABLE 3** Primary antibodies

Target	Catalog nr	Company	Species	Dilution
$\alpha$ SMA	M0851	Dako	Mouse	1:1000
FN	ab2413	Abcam	Rabbit	1:1000
EP <sub>2</sub>	ab167171	Abcam	Rabbit	1:500
Smad2	5339	Cell Signalling	Rabbit	1:1000
pSmad2	3108	Cell Signalling	Rabbit	1:1000

tissue), both supplemented with phosphatase-inhibitor 2 and 3 and a mini protease inhibitor tablet. Afterwards, 2% SDS and DTT were added to the samples, and they were heated for 15 min at 65°C. Total protein was separated by SDS/PAGE using 12% Criterion TGX Stain-free gels and subsequently blotted onto a nitrocellulose membrane. Afterwards, the membrane was blocked for 1 h with 5% skimmed milk in PBS-T. The blot was then incubated overnight at 4°C with specific primary antibodies (Table 3). Afterwards, the membrane was washed with PBS-T and incubated with the appropriate secondary antibody for 1 h at RT. Binding of the antibodies was visualized using ECL-prime.

#### 4.8 | Immunolabeling

Kidneys were fixed by perfusion through the left ventricle using 4% paraformaldehyde (PFA) in water. Afterwards, kidneys were immersed in 4% PFA for 1 h, rinsed with PBS, dehydrated using a graded series of alcohol and embedded in paraffin. Subsequently, tissue sections (2  $\mu$ M) were deparaffinized, rehydrated, and then boiled in TEG-buffer for 16 min for epitope retrieval. Hereafter, sections were left to cool, and then incubated for 30 min in 50 mM NH<sub>4</sub>Cl to block free aldehyde groups. Afterwards, sections were incubated with blocking solution (PBS containing 1% BSA, 0.2% gelatin and 0.05% saponin) for 30 min. For immunoperoxidase labelling, the sections were incubated with a primary antibody against EP<sub>2</sub> (Table 3) diluted in PBS with 0.1% BSA and 0.3% Triton-X-100 overnight at 4°C. Subsequently, the sections were washed three times with PBS containing 0.1% BSA, 0.2% gelatin and 0.05% saponin followed by incubation with a P448 secondary antibody diluted in washing solution for 1 h at RT. Afterwards, the sections were rinsed with PBS wash-buffer, and the sites of antibody-antigen reactions were visualized with 0.05% 3,3'-diaminobenzidine tetrahydrochloride (Kem-En-Tec, Copenhagen, Denmark) dissolved in distilled water containing 0.1% H<sub>2</sub>O<sub>2</sub>. Light microscopy was performed using an Olympus BX50 light microscope and CellSens imaging software.

For immunofluorescence labelling, sections were covered with mouse-on-mouse blocking solution containing unconjugated AffiniPure Fab Fragment Donkey Anti-Mouse IgG (Jackson ImmunoResearch) in PBS for 1 h at RT and then

fixed for 10 min in 4% PFA. Sections were incubated overnight at 4°C with primary antibodies (EP<sub>2</sub> and  $\alpha$ SMA, Table 3) diluted in PBS containing 0.1% BSA and 0.3% Triton X-100. Sections were subsequently washed for 30 min in PBS containing 0.1% BSA, 0.2% gelatin, and 0.05% saponin and then incubated with Alexa Fluor 488 and Alexa Fluor 568-conjugated secondary antibody at RT for 30 min (Life Technologies). Then, sections were counterstained with 4,6-diamidino-2-phenylindole (DAPI), washed with PBS, and mounted with SlowFade Gold Antifade Mountant (Life Technologies). Fluorescence microscopy was performed using an Olympus BX61 microscope and image processing was performed using Xcellence Rt software.

In addition, sections were stained with hematoxylin and eosin to assess kidney damage and tubular dilation. In order to evaluate tubule volume, a grid overlay was placed on each picture and tubules located at the points of intersections were marked. Afterwards, the lumen was measured in percentages of the marked area. Five pictures were captured in a blinded manner from each specimen at x20 magnification with no overlapping regions, and 6 tubules were assessed in each picture. Interstitial volume was calculated using ImageJ software based on signal intensity of the  $\alpha$ SMA immunolabeling.

#### 4.9 | PCR

Total RNA was isolated using either TRIzol Reagent (cells) or a NucleoSpin RNA II mini kit (kidney tissue; Macherey Nagel), following the manufacturer's instructions. RNA was quantitated by spectrophotometry and stored at -80°C. cDNA was synthesized from 0.5  $\mu$ g RNA with the RevertAid First Strand synthesis kit (Thermo Scientific). To confirm expression of the EP<sub>2</sub> receptor in MDCK cells, RT-PCR was performed with (+) or without (-) reverse transcriptase (RT) enzyme. Afterwards, the PCR product was analysed by electrophoresis using a 1% agarose gel run at 70 V for 45 min, including a marker (Generuler DNA marker, Invitrogen). Images of the gel were obtained with an Azure c200 gel imaging workstation. To study the expression level of the other genes of interest, qPCR was performed using 100 ng cDNA, which served as the template for PCR amplification using the Brilliant SYBR Green qPCR Master Mix (Thermo Scientific), according to the manufacturer's instructions. Used primers are listed in Table 4.

#### 4.10 | Statistics

Statistics were performed using Graphpad Prism by either one-way ANOVA followed by Tukey's or Dunnett's multiple comparisons test, two-way ANOVA followed by Tukey's post hoc test or using an unpaired two-tailed Student's t test as appropriate. Differences between groups were considered to be statistically significant when  $P < 0.05$ .

TABLE 4 Primer sequences

Target gene	Accession number	Forward	Reverse
<i>Murine</i>			
$\alpha$ SMA	NM_007392.3	5'-CTGACAGAGGCCACCACTGAA-3'	5'-CATCTCCAGAGTCCAGCACA-3'
FN	NM_010233.2	5'-AATGGAAAAGGGGAATGGAC-3'	5'-CTCGGTTGTCCTTCTTGCTC-3'
EP <sub>2</sub>	NM_008964.4	5'-ATGCTCCTGCTGCTTATCGT-3'	5'-AGGGCCTCTTAGGCTACTGC-3'
COL1A1	NM_007742.4	5'-CACCTCAAGAGCCTGAGTC-3'	5'-ACTCTCCGCTCTTCCAGTCA-3'
18S	NM_011296.2	5'-GAAAATAGCCTTCGCCATCA-3'	5'-TCCATCCTTCACATCCTTC-3'
<i>Human</i>			
EP <sub>2</sub>	NM_000956.3	5'-CCACCTCATTCTCCTGGCTA-3'	5'-TTCTTTTCGGGAAGAGGTTT-3'
$\alpha$ SMA	NM_001141945.2	5'-ACCCACAATGTCCCCATCTA-3'	5'-GAAGGAATAGCCACGCTCAG-3'
FN	NM_212482.2	5'-CAGTGGGAGACCTCGAGAAG-3'	5'-GTCCCTCGGAACATCAGAAA-3'
COL1A1	NM_000088.3	5'-CCTGGATGCCATCAAAGTCT-3'	5'-AATCCATCGGTCATGCTCTC-3'
RPL22	NM_000983.3	5'-TCGCTCACCTCCCTTCTAA-3'	5'-TCACGGTGATCTTGCTCTTG-3'
GAPDH	NM_002046.5	5'-ACCAGGGCTGCTTTTAACTCT-3'	5'-GGTGCCATGGAATTTGCC-3'
<i>Canine</i>			
TGF $\beta$	NM_001003309.1	5'-AAGAAAAGTCCGCACAGCAT-3'	5'-GCTGCTCCGCTTTTAACTTG-3'
GAPDH	NM_001003142.2	5'-AACATCATCCCTGCTTCCAC-3'	5'-GGCAGGTCAGATCCACAAC-3'

## ACKNOWLEDGEMENTS

The authors thank Gitte Skou and Gitte Kall for expert technical assistance. We also would like to thank the surgeons at the Department of Urology, Aarhus University Hospital for providing human tissue samples. This work was kindly supported by Lundbeckfonden, grant number R231-2016-2344 (received by H.A.M.M.) as well as the Danish Council for Independent Research, grant number 6110-00231B, Aarhus University Research Foundation, grant number AUFF-E-2015-FLS-8-69 and Hildur and Dagny Jacobsens Foundation grant number 1295716-1 (received by R.N.).

## CONFLICT OF INTEREST

The authors have declared that no conflict of interest exists.

## AUTHORS' CONTRIBUTIONS

MSJ, HAMM and RN designed the study; MSJ, HAMM, SJT, MC, TK and RN carried out experiments and analysed the data; PO provided additional analytical tools and chemicals for this study; MGM helped with human tissue procurement; MSJ, HAMM and RN wrote the manuscript with critical review from SJT, MC, MGM, PO and TK. All of the authors approved the final version of the manuscript for publication.

## ORCID

Rikke Nørregaard  <https://orcid.org/0000-0002-0580-373X>

## REFERENCES

- Jha V, Garcia-Garcia G, Iseki K, et al. Chronic kidney disease: global dimension and perspectives. *Lancet*. 2013;382(9888):260-272.
- Liu Y. Renal fibrosis: new insights into the pathogenesis and therapeutics. *Kidney Int*. 2006;69(2):213-217.
- Norregaard R, Kwon TH, Frokiaer J. Physiology and pathophysiology of cyclooxygenase-2 and prostaglandin E2 in the kidney. *Kidney Res Clin Pract*. 2015;34(4):194-200.
- Nilsson L, Madsen K, Krag S, Frokiaer J, Jensen BL, Norregaard R. Disruption of cyclooxygenase type 2 exacerbates apoptosis and renal damage during obstructive nephropathy. *Am J Physiol Renal Physiol*. 2015;309(12):F1035-F1048.
- Yang C, Nilsson L, Cheema MU, et al. Chitosan/siRNA nanoparticles targeting cyclooxygenase type 2 attenuate unilateral ureteral obstruction-induced kidney injury in mice. *Theranostics*. 2015;5(2):110-123.
- Breyer MD, Zhang Y, Guan YF, Hao CM, Hebert RL, Breyer RM. Regulation of renal function by prostaglandin E receptors. *Kidney Int Suppl*. 1998;67:S88-S94.
- Thibodeau J-F, Nasrallah R, Carter A, et al. PTGER1 deletion attenuates renal injury in diabetic mouse models. *Am J Pathol*. 2013;183(6):1789-1802.
- Kennedy C, Zhang Y, Brandon S, et al. Salt-sensitive hypertension and reduced fertility in mice lacking the prostaglandin EP2 receptor. *Nat Med*. 1999;5(2):217-220.
- Nakagawa N, Yuhki K-I, Kawabe J-I, et al. The intrinsic prostaglandin E2-EP4 system of the renal tubular epithelium limits the development of tubulointerstitial fibrosis in mice. *Kidney Int*. 2012;82(2):158-171.
- Kolodnick JE, Peters-Golden M, Larios J, Toews GB, Thannickal VJ, Moore BB. Prostaglandin E2 inhibits fibroblast to myofibroblast transition via E. prostanoid receptor 2 signaling and cyclic adenosine monophosphate elevation. *Am J Respir Cell Mol Biol*. 2003;29(5):537-544.

11. Lee SY, Kim SI, Choi ME. Therapeutic targets for treating fibrotic kidney diseases. *Transl Res*. 2015;165(4):512-530.
12. Liu J, Zhang YD, Chen XL, et al. The protective effect of the EP2 receptor on TGF-beta1 induced podocyte injury via the PI3K / Akt signaling pathway. *PLoS ONE*. 2018;13(5):e0197158.
13. Xi PP, Xu YY, Chen XL, Fan YP, Wu JH. Role of the prostaglandin E2 receptor agonists in TGF-beta1-induced mesangial cell damage. *Biosci Rep*. 2016;36(5):e00383.
14. Lovisa S, LeBleu VS, Tampe B, et al. Epithelial-to-mesenchymal transition induces cell cycle arrest and parenchymal damage in renal fibrosis. *Nat Med*. 2015;21(9):998-1009.
15. Galichon P, Finianos S, Hertig A. EMT-MET in renal disease: should we curb our enthusiasm? *Cancer Lett*. 2013;341(1):24-29.
16. Xu-Dubois Y-C, Baugey E, Peltier J, et al. Epithelial phenotypic changes are associated with a tubular active fibrogenic process in human renal grafts. *Hum Pathol*. 2013;44(7):1251-1261.
17. Black SA Jr, Trackman PC. Transforming growth factor-beta1 (TGFbeta1) stimulates connective tissue growth factor (CCN2/CTGF) expression in human gingival fibroblasts through a RhoA-independent, Rac1/Cdc42-dependent mechanism: statins with forskolin block TGFbeta1-induced CCN2/CTGF expression. *J Biol Chem*. 2008;283(16):10835-10847.
18. Liu X, Li F, Sun SQ, et al. Fibroblast-specific expression of AC6 enhances beta-adrenergic and prostacyclin signaling and blunts bleomycin-induced pulmonary fibrosis. *Am J Physiol Lung Cell Mol Physiol*. 2010;298(6):L819-L829.
19. Olesen ET, Moeller HB, Assentoft M, MacAulay N, Fenton RA. The vasopressin type 2 receptor and prostaglandin receptors EP2 and EP4 can increase aquaporin-2 plasma membrane targeting through a cAMP-independent pathway. *Am J Physiol Renal Physiol*. 2016;311(5):F935-F944.
20. Neil JR, Johnson KM, Nemenoff RA, Schiemann WP. Cox-2 inactivates Smad signaling and enhances EMT stimulated by TGF-beta through a PGE2-dependent mechanisms. *Carcinogenesis*. 2008;29(11):2227-2235.
21. Tian M, Schiemann WP. PGE2 receptor EP2 mediates the antagonistic effect of COX-2 on TGF-beta signaling during mammary tumorigenesis. *FASEB J*. 2010;24(4):1105-1116.
22. Yang C, Chen C, Sorokin A. Prostaglandin E2 modifies SMAD2 and promotes SMAD2-SMAD4 complex formation. *Prostaglandins Leukot Essent Fatty Acids*. 2014;90(5):145-149.
23. Breyer MD, Breyer RM. Prostaglandin E receptors and the kidney. *Am J Physiol Renal Physiol*. 2000;279(1):F12-F23.
24. Guan Y, Stillman BA, Zhang Y, et al. Cloning and expression of the rabbit prostaglandin EP2 receptor. *BMC Pharmacol*. 2002;2:14.
25. Jensen BL, Stubbe J, Hansen PB, Andreasen D, Skott O. Localization of prostaglandin E(2) EP2 and EP4 receptors in the rat kidney. *Am J Physiol Renal Physiol*. 2001;280(6):F1001-F1009.
26. Hruska KA, Guo G, Wozniak M, et al. Osteogenic protein-1 prevents renal fibrogenesis associated with ureteral obstruction. *Am J Physiol Renal Physiol*. 2000;279(1):F130-F143.
27. Stribos E, Luangmonkong T, Leliveld AM, et al. Precision-cut human kidney slices as a model to elucidate the process of renal fibrosis. *Transl Res*. 2016;170:8-16.e1.

**How to cite this article:** Jensen MS, Mutsaers HAM, Tingskov SJ, et al. Activation of the prostaglandin E<sub>2</sub> EP<sub>2</sub> receptor attenuates renal fibrosis in unilateral ureteral obstructed mice and human kidney slices. *Acta Physiol*. 2019;227:e13291. <https://doi.org/10.1111/apha.13291>